

Translucent Nanoparticle-Based Aerogel Monoliths as 3-Dimensional Photocatalysts for the Selective Photoreduction of CO₂ to Methanol in a Continuous Flow Reactor

*Felix Rechberger and Markus Niederberger**

Laboratory for Multifunctional Materials, Department of Materials, ETH Zurich, Vladimir-Prelog-Weg 5, CH-8093 Zurich, Switzerland.

E-mail: markus.niederberger@mat.ethz.ch

Electronic Supplementary Information

Experimental details

Chemicals

Titanium (IV) tetrachloride (99.9 % trace metals basis), benzyl alcohol (puriss., 99-100.5 % (GC)), 2-amino-2-(hydroxymethyl)-1,3-propanediol (Trizma[®] base, puriss., ≥ 99.7 %), sodium citrate dihydrate (≥ 99 %), chloroform (≥ 99.8 %), diethyl ether (for HPLC, ≥ 99.9 %, inhibitor-free), deuterium oxide (99.96 at.% D), ammonium hydroxide solution (25% in water, extra pure), ethanol (absolute) and acetone (for HPLC ≥99.8 %) were purchased from Sigma-Aldrich. Gold (III) chloride (99 %) was purchased from Acros. Liquid carbon dioxide (≥ 99 %), carbon dioxide (99.9 %), nitrogen (99,999 %), argon (99.999 %), helium (99,999 %) and various calibration gases were provided by PanGas AG, Switzerland. All chemicals were used as received without further purification.

Preparation of nanoparticles

Trizma-functionalized anatase nanoparticles were synthesized by an upscaled and modified route by Niederberger *et al.*,^{1,2} which was previously used in our group for TiO₂ based aerogels.³⁻⁶

414 mg (3.4 mmol) Trizma were dissolved in 90 mL benzyl alcohol at 80 °C in an oil bath. After cooling to room temperature, 4.5 mL (40.9 mmol) titanium (IV) chloride were added under vigorous stirring and the reaction solution was heated at 80 °C for 24 h. The white precipitate was separated from the solution by centrifugation and washed three times with chloroform and subsequently three times with diethyl ether.

The gold nanoparticles were synthesized according to the route of Turkevich *et al.*⁷ 77.1 mg (0.263 mmol) sodium citrate tribasic dihydrate were dissolved in 300 mL deionized water and heated in an oil bath with the temperature set to 120 °C. As the solution started boiling, 25.5 mg (0.075 mmol) gold chloride was added and the solution was refluxed for 24 h. The calculated gold concentration in the final solution was 0.049 g L⁻¹ (0.25 mmol L⁻¹).

Dispersion and gelling

The white and wet precipitate was dispersed in 30 mL deionized water for pure anatase gels or in 30 mL of prepared aqueous gold solution for anatase-gold composite aerogels and by applying a vacuum, the residual diethylether was removed. The aqueous dispersion of nanoparticles was diluted by 100 % with ethanol and transferred to prepared 10 mL syringes cut open and heated to 60 °C for 30 min in a saturated ethanol atmosphere to induce gelation, similar to a previously published protocol.⁴ The translucent monolithic gels were immediately immersed into an ethanol-water mixture to avoid drying and cracking. Subsequently, the pore liquid was gradually exchanged to acetone in 20 vol. % steps, each lasting ≥ 12 h. Finally, the acetone was removed under full preservation of the microstructure by supercritical drying in a Tousimis 931 GL.

Characterization

Powder X-ray diffraction (XRD) was measured on a PANalytical Empyrean equipped with a PIXcel 1D detector and Cu K α X-ray irradiation. By using the Scherrer equation on the (101) reflection, mean crystallite sizes were calculated by using the effect of peak broadening. For the microstructural characterization, scanning electron microscopy (SEM) was performed on a Hitachi SU-70 operated at 5 kV. Surface organics were characterized by attenuated total reflection Fourier transformed infrared spectroscopy (ATR-FTIR) recorded on a Bruker ALPHA FT-IR spectrophotometer.

Gas sorption experiments were performed on a Quantachrome Autosorb iQ. Before the analyses with nitrogen at 77 K, the samples were outgassed at 100 °C for at least 24 h. The surface area was determined *via* the Brunauer-Emmet-Teller (BET) method and the pore size and pore volume were determined by density functional theory (DFT) analysis using a Non Local DFT (NLDFIT) calculation model for nitrogen at 77 K on silica cylindrical pores.⁸

UV-vis spectra were obtained on a JASCO V-770 spectrophotometer equipped with an ILN-725 integrating sphere with background subtraction. Aerogel samples were specifically produced in different thicknesses and placed on a black cardboard frame prior to analysis.

The photocatalytic gas phase reactions were performed in a custom made continuous flow reactor with the aerogel monolith fixed within a quartz tube (Robson Scientific, 14 mm inner diameter) by Teflon centering rings and NBR o-rings to ensure gas tightness. CO₂ gas was bubbled through a bath at room temperature to enrich with humidity or any other liquid vapor at a flow rate of 5 mL min⁻¹, which was controlled by a mass flow meter (Cole-Parmer) and a needle valve (VICI® Valco Instruments Co. Inc.). Finally, the gas was directed to the quartz tube via custom build ISO-KF connectors (see Figure S1 for the different reactor components). Pressure differences were measured on a digital manometer LEO 2 (Keller). The sample was equilibrated for 3 h in the dark under continuous flow prior to the measurements.

Simulated solar irradiation was provided by a Newport solar simulator equipped with a 300 W Xe lamp operated at 266 W. The intensity was adjusted to 100 mWcm^{-1} with neutral density filters and an AM 1.5 G filter. A 415 nm long pass filter was used to remove shortwave UV irradiation to test the photoactivity under absence of UV light. The gas products were analyzed by means of mass spectrometry (MS) and gas chromatography (GC). Mass spectra for qualitative measurements in the range of $1\text{-}200 \text{ m z}^{-1}$ were recorded at 100 ms amu^{-1} on a Thermostar GSD 320 (Pfeiffer Vacuum) equipped with a quadrupole mass analyzer and a Faraday cup detector. GC for qualitative and quantitative measurements were performed on an Inficon Micro-GC 3000A, equipped with He and Ar carrier gases and four separate modules, each consisting of an individual injector system, column and μ -TCD detector: twice $10 \text{ m Molsieve} \times 30 \mu\text{m}$, $8 \text{ m PLOT Q}/1\text{m PLOT Q} \times 10 \mu\text{m}$ with backflush injector and $20 \text{ m OV-1} \times 2 \mu\text{m}$. Samples were taken every 5 minutes and moisture droplets were removed by a Genie membrane filter G2870A-01. Various calibration gases were used to calibrate the GC.

Figures



Figure S1 Photograph of the different reactor components with half of the setup assembled.

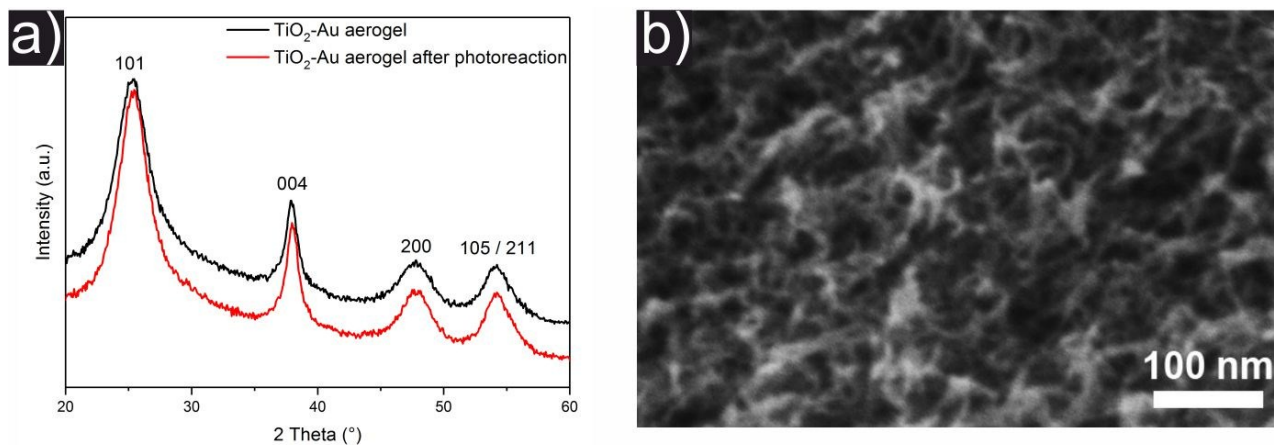


Figure S2 Characterization of the TiO₂-Au aerogel: a) XRD pattern with peaks ascribed to anatase TiO₂ (ICDD PDF No. 1-70-6826) and b) scanning electron micrograph depicting the porous network of the sample.

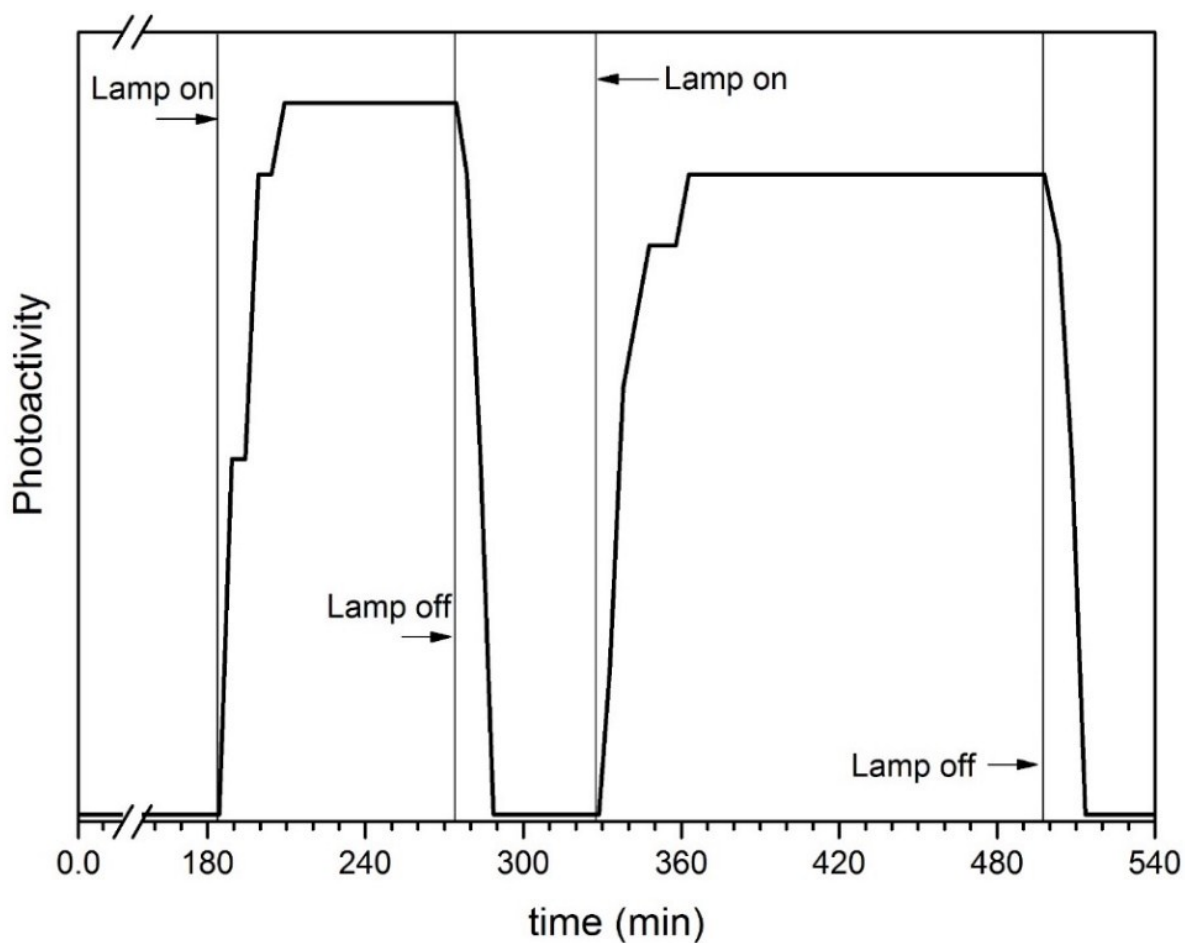


Figure S3 Photoactivity of the TiO₂-Au aerogel under chopped illumination.

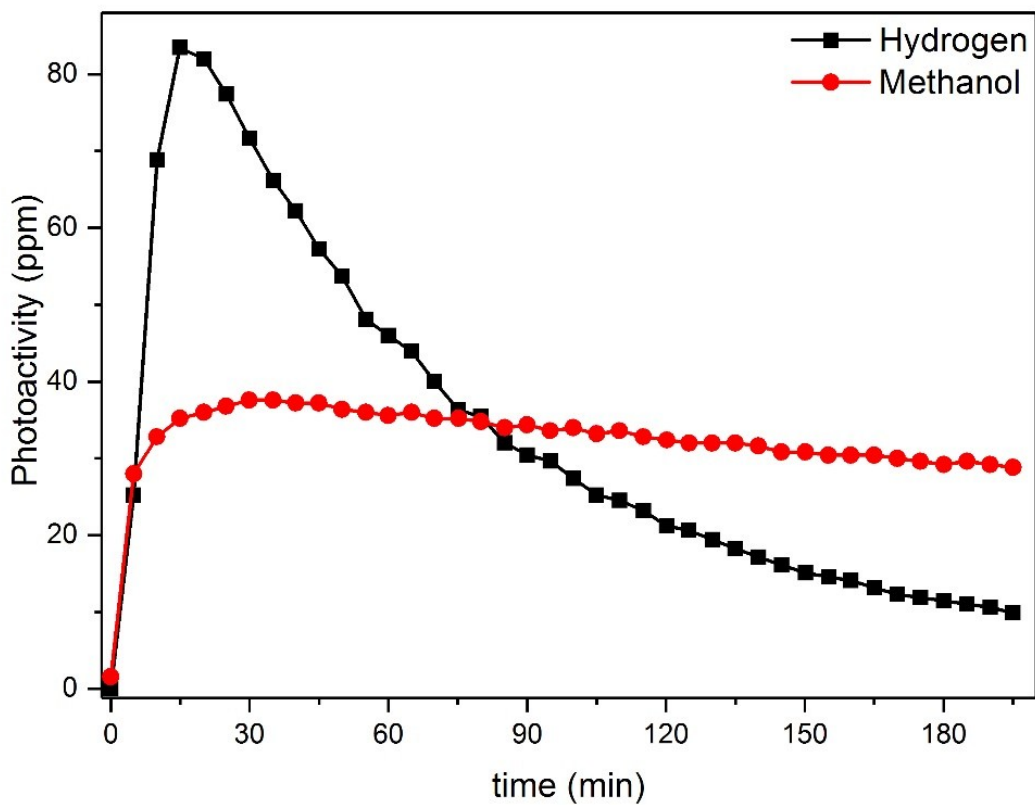


Figure S4 Photoactivity of the TiO₂-Au aerogel under the release of hydrogen originating from the decomposition of Trizma and the production of methanol by photoreducing CO₂ with H₂O.

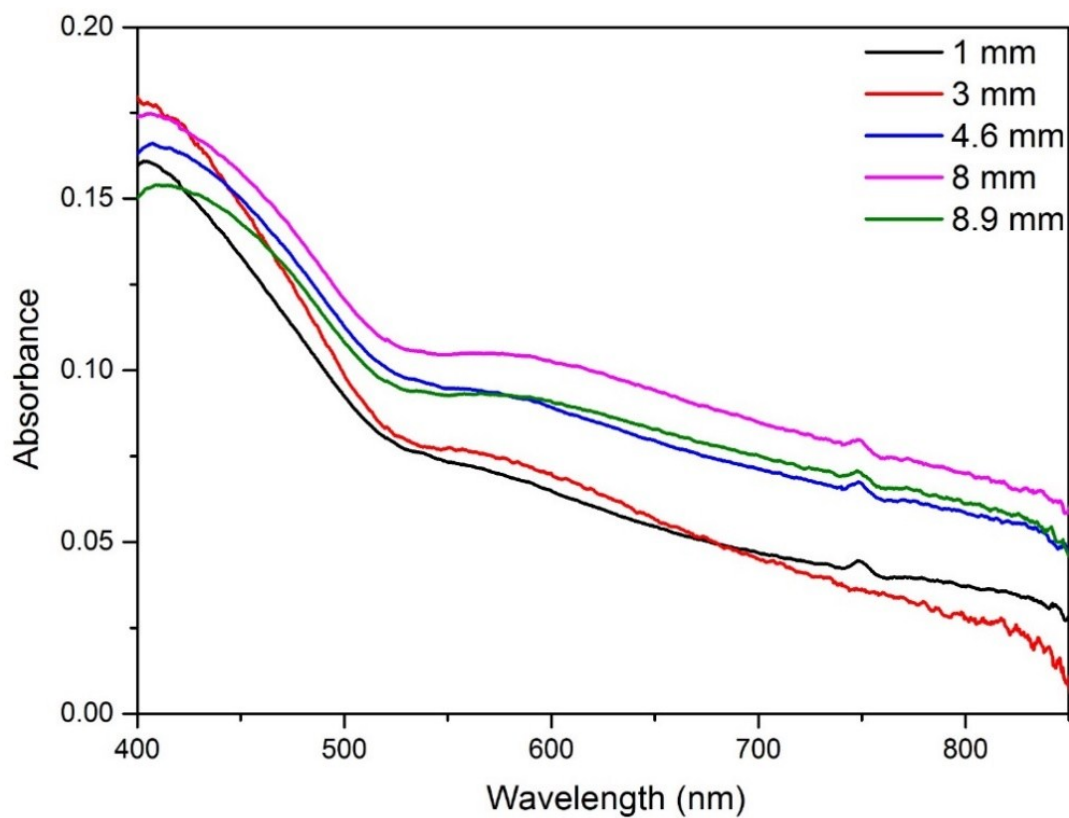


Figure S5 Diffuse reflectance spectra for different TiO₂-Au aerogel thicknesses.

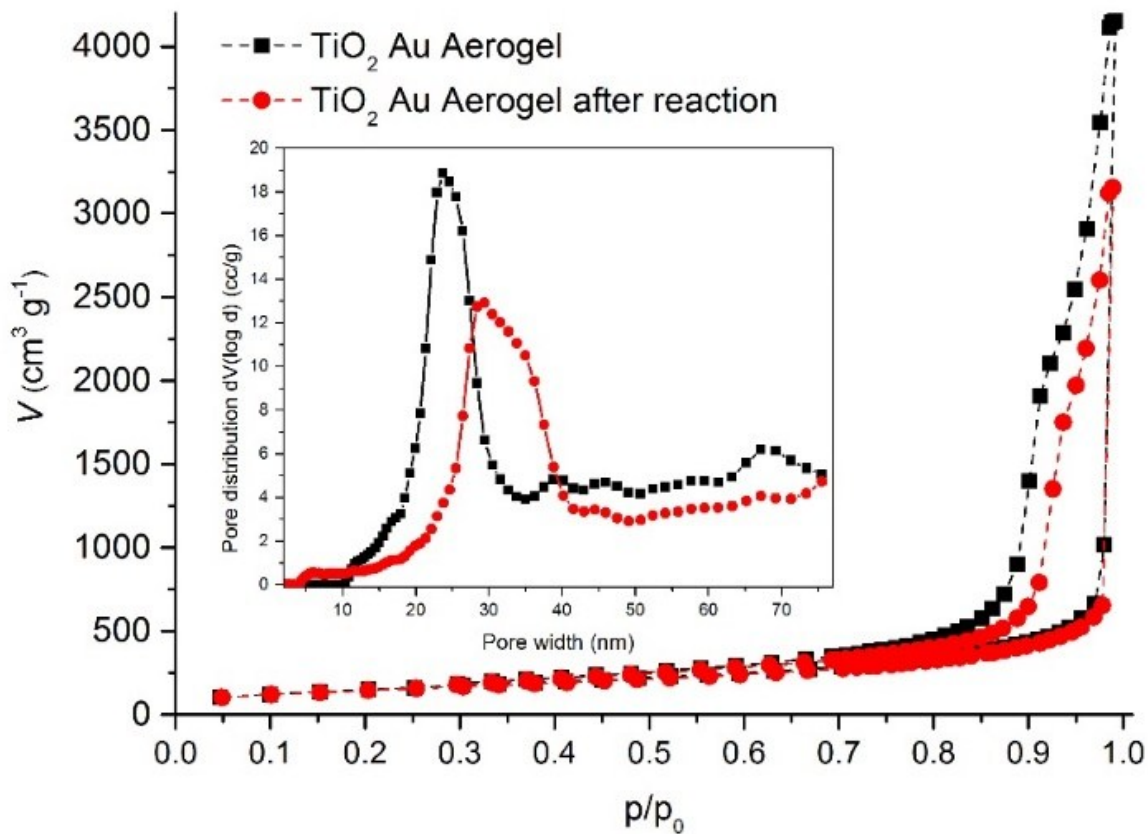


Figure S6 N₂ gas sorption isotherms for TiO₂-Au composite aerogel samples before (black squares) and after (red circles) the reaction. The inset shows the shift in pore size distribution occurring after the reaction.

References

1. J. Polleux, N. Pinna, M. Antonietti and M. Niederberger, *Adv. Mater.*, 2004, **16**, 436-439.
2. J. Polleux, N. Pinna, M. Antonietti, C. Hess, U. Wild, R. Schlögl and M. Niederberger, *Chem. Eur. J.*, 2005, **11**, 3541-3551.
3. F. J. Heiligtag, M. D. Rossell, M. J. Süess and M. Niederberger, *J. Mater. Chem.*, 2011, **21**, 16893-16899.
4. F. J. Heiligtag, M. J. I. Airaghi Leccardi, D. Erdem, M. J. Süess and M. Niederberger, *Nanoscale*, 2014, **6**, 13213-13221.
5. F. J. Heiligtag, W. Cheng, V. R. de Mendonça, M. J. Süess, K. Hametner, D. Günther, C. Ribeiro and M. Niederberger, *Chem. Mater.*, 2014, **26**, 5576-5584.
6. F. J. Heiligtag, N. Kränzlin, M. J. Süess and M. Niederberger, *J. Sol-Gel Sci. Technol.*, 2014, **70**, 300-306.
7. J. Kimling, M. Maier, B. Okenve, V. Kotaidis, H. Ballot and A. Plech, *J. Phys. Chem. B*, 2006, **110**, 15700-15707.
8. J. Landers, G. Y. Gor and A. V. Neimark, *Colloids Surf., A*, 2013, **437**, 3-32.